Chemosphere 82 (2011) 1489–1495

Contents lists available at ScienceDirect

Chemosphere

journal homepage: www.elsevier.com/locate/chemosphere

Role of microbial exopolymeric substances (EPS) on chromium sorption and transport in heterogeneous subsurface soils: I. Cr(III) complexation with EPS in aqueous solution

Cetin Kantar [a,*], Hilal Demiray [a], Nazime Mercan Dogan [b], Cleveland J. Dodge [c]

[a] Mersin University, Faculty of Engineering, Department of Environmental Engineering, Mersin, Turkey
[b] Pamukkale University, Faculty of Arts and Science, Department of Biology, Denizli, Turkey
[c] Environmental Sciences Department, Brookhaven National Laboratory, Uptown, NY 11973, USA

ARTICLE INFO

Article history:
Received 3 September 2010
Received in revised form 31 December 2010
Accepted 2 January 2011
Available online 26 January 2011

Keywords:
Chromium
Discrete ligand model
Complexation
EPS
Speciation
Transport

ABSTRACT

Chromium (III) binding by exopolymeric substances (EPS) isolated from *Pseudomonas putida* P18, *Pseudomonas aeruginosa* P16 and *Pseudomonas stutzeri* P40 strains were investigated by the determination of conditional stability constants and the concentration of functional groups using the ion-exchange experiments and potentiometric titrations. Spectroscopic (EXAFS) analysis was also used to obtain information on the nature of Cr(III) binding with EPS functional groups. The data from ion-exchange experiments and potentiometric titrations were evaluated using a non-electrostatic discrete ligand approach. The modeling results show that the acid/base properties of EPSs can be best characterized by invoking four different types of acid functional groups with arbitrarily assigned pK_a values of 4, 6, 8 and 10.

The analysis of ion-exchange data using the discrete ligand approach suggests that while the Cr binding by EPS from *P. aeruginosa* can be successfully described based on a reaction stoichiometry of 1:2 between Cr(III) and HL_2 monoprotic ligands, the accurate description of Cr binding by EPSs extracted from *P. putida* and *P. stutzeri* requires postulation of 1:1 Cr(III)-ligand complexes with HL_2 and HL_3 monoprotic ligands, respectively. These results indicate that the carboxyl and/or phosphoric acid sites contribute to Cr(III) binding by microbial EPS, as also confirmed by EXAFS analysis performed in the current study.

Overall, this study highlights the need for incorporation of Cr–EPS interactions into transport and speciation models to more accurately assess microbial Cr(VI) reduction and chromium transport in subsurface systems, including microbial reactive treatment barriers.

1. Introduction

Microbial exopolymeric substances (EPS) are one of the major components of natural organic matter (NOM) in natural systems. Exopolymeric substances (EPS) are produced by microbes for a variety of purposes in response to environmental stresses e.g., pH. Quantity and composition of EPS have been shown to vary depending upon bacterial strain and environmental stresses (e.g., pH, temperature, toxic metal ions) in several studies (e.g., Aquino and Stuckey, 2004; Guibaud et al., 2005; Sheng et al., 2005; Priester et al., 2006). For example, in a study with the hydrogen-producing photosynthetic bacteria strain *Rhodopseudomonas acidophila*, Sheng et al. (2005) found that toxic substances such as chromium (VI) stimulated the production of microbial EPS. Similarly, in anaerobic chemostats fed on glucose, Aquino and Stuckey (2004) observed that exposure to excess Cr(VI) led to an enhanced EPS production.

Recently, a number of researchers have reported on the effects of microbial EPS on chromium speciation and behavior in natural systems. For example, Priester et al. (2006) found that chromium (III) that formed after microbial reduction of Cr(VI) with *Pseudomonas putida* was partly associated with exoplymeric substances (EPS). Puzon et al. (2005) found that Cr(VI) reduction in the presence of cellular organic metabolites (e.g., citrate, ascorbate, malate) formed highly soluble organo-Cr(III) complexes, which are very stable over a broad pH range. Similarly, Cetin et al. (2009) found that EPS constituents such as alginic and galacturonic acids lowered Cr(III) sorption to soils due to the formation of highly soluble and less sorbing Cr(III)-ligand complexes between functional groups (e.g., carboxylic) of EPS and Cr(III).

Microbial EPSs contain multiple functional groups (e.g., carboxylic, phosphate, amine, hydroxylic functional groups) for binding with metal ions e.g., Cr (Guibaud et al., 2008). The nature of proton and metal binding by EPS varies with the type and composition of EPS (Priester et al., 2006). For example, while Lamelas et al. (2006) accurately described the acid/base characteristics of EPS isolated from *Rhizobium meliloti* using two different pK_a values (pK_{a1} 3.4

* Corresponding author. Tel.: +90 324 361 0001x7092; fax: +90 324 361 0032.
E-mail address: ckantar@mersin.edu.tr (C. Kantar).

0045-6535/$ - see front matter © 2011 Elsevier Ltd. All rights reserved.
doi:10.1016/j.chemosphere.2011.01.009

and pK_{a2} 6.17), Liu and Fang (2002) found that at least 6 different pK_a values (4.4, 6.0, 7.4, 8.2, 9.4 and 11) were required to represent all functional groups found in microbial EPS extracted from sulfate reducing bacteria. Similarly, Comte et al. (2008) determined 2 distinct pK_a values for EPSs isolated from activated sludge. Studies by Guibaud et al. (2005) and Tourney et al. (2009) indicate that the carboxyl and phosphate functional groups play an important role on metal ion binding by EPS due to high P and COOH contents of microbial EPS.

Metal–EPS interactions have been modeled predominantly through the use of graphical techniques such as those of Schubert's (Schubert, 1948), Kurbatov's (Kurbatov et al., 1951) and (Ruzic, 1996) (e.g., Guibaud et al., 2003, 2005, 2006). As stated by Harper et al. (2008), graphical techniques work well for complexes with relatively simple stoichiometries in terms of metal-ion: ligand ratios (e.g., 1:1; 1:2) but can be problematic when mixed stoichiometries exist (e.g., a mixture of 1:1 and 1:2 complexes (Smith et al., 1986)). An alternative avenue is the use of chemical models that describe metal and proton binding by EPS through the use of a discrete ligand or a distribution of ligands with or without the inclusion of electrostatic effects (e.g., Westall et al., 1995; Lamelas et al., 2006). A characteristic of the use of chemical speciation models is the emphasis on the development of a molecular hypothesis for the complexant. In this study, a comparison of Cr complexation by EPS produced by three bacterial strains, we conceptualize the protolytic characteristics of EPS as being represented as a linear combination of independent, ionogenic sites. This is an approach described by Westall et al. (1995) and later used by several researchers (e.g., Kantar and Honeyman, 2005; Harper et al., 2008).

Although there is substantial evidence on the production of microbial EPS during microbial Cr(VI) reduction, little is known about specific interactions between Cr(III) and EPS released by bacteria. The purpose of this current study was to determine the effects of microbial EPS on Cr speciation and subsequent mobility or immobility in subsurface systems contaminated with Cr. The nature of Cr(III) complexation with EPS functional groups and Cr: ligand reaction stoichiometries were investigated for three different microbial EPSs isolated from *P. putida* P18, *Pseudomonas stutzeri* P40 and *Pseudomonas aeruginosa* P16. The extent of Cr complexation with the EPS functional groups was evaluated using a combination of a ligand competition technique employing a cation exchange technique and X-ray Absorption Fine Structure (EXAFS) Spectroscopy. Potentiometric titration and Cr–EPS complexation data were evaluated using a non-electrostatic discrete model in FITEQL (Herbelin and Westall, 1999). While the application of non-electrostatic discrete ligand models to the interpretation of complexation data is not new in the literature (e.g., Kantar and Honeyman, 2005), it is not common, especially in complex systems involving microbial EPS. In addition, the development of such simple mechanistic modeling approaches allows the modelers to incorporate metal–ligand interactions (e.g., Cr–EPS complexation) into surface complexation (SCM) and reactive transport models. In Part 2 of this publication series (Kantar et al., 2010), for instance, we show that the discrete ligand model developed for the description of Cr–EPS interactions in the current study can be easily incorporated into a non-electrostatic SCM to accurately simulate the effects of EPS on Cr(III) sorption and transport in heterogeneous subsurface soils under a wide range of environmental conditions (e.g., pH).

2. Materials and methods

2.1. Materials

Unless stated otherwise, all chemicals used in the experiments were reagent grade or better. Water for all experiments was supplied from Millipore (Simplicity 185) UV (ultraviolet)-water system. Chromium (III)-nitrate-nanohydrate (Merck) was used as the source for Cr(III) in all experiments. DOWEX 50WX8-200 cation exchange resin, cleaned and treated as described in Kantar and Honeyman (2005) was used in all resin exchange experiments. To precondition the internal surfaces, Oak Ridge type centrifuge tubes used for ion-exchange experiments were soaked in 0.01 M NaCl solution, rinsed and allowed to dry. All stock solutions, including NaOH and HCl for pH adjustments, NaCl for ionic strength adjustment were prepared using UV-water and stored in amber glass bottles in the dark at 4 °C.

Stock solutions of 'dissolved EPS' were prepared using EPSs isolated from *P. aeruginosa* P16, *P. putida* P18, and *P. stutzeri* P40 as described by Hung et al. (2005). Total carbohydrate contents of EPS were measured by the phenol–sulfuric acid method using glucose as the standard (Southgate, 1976). Total protein was quantified by a modified Lowry method (Hartree, 2004). Total concentrations of uronic acids in EPSs were determined by a spectrophotometric method, as modified by Hung and Santschi (2001). The phosphorus contents of dissolved EPS were analyzed with ICP-MS. Detailed information regarding EPS isolation and purification from bacteria can be found in Supporting information, page S2.

2.2. Potentiometric titrations

Potentiometric titrations of the three EPS isolates were performed in a temperature-controlled glass cell (24 ± 2 °C) under a CO_2 free atmosphere using an automated computer controlled titrimeter to determine EPS acid–base characteristics. The titrations were conducted with HCl and NaOH titrants (CO_2-free), standardized against potassium hydrogen phthalate. Appropriate aliquots of NaCl and UV-water were added to the cell to bring the sample to 50 mL and the desired ionic strength. The titrations were performed at ionic strengths of 0.01 and 0.1 M NaCl. The samples containing EPS were first acidified with HCl, and sparged slowly with N_2 gas for an hour to remove CO_2 gas. Titrations were performed at EPS concentrations of 325, 385 and 397.5 mg L^{-1} for *P. stutzeri* P40, *P. putida* P18 and *P. aeruginosa* P16, respectively. The solutions were titrated first with 0.1 N NaOH from an initial pH of 3.0 to a final pH of 10.5, and then titrated back to pH 3.0 with 0.1 N HCl.

2.3. Ion-exchange experiments

A series of ion-exchange experiments were conducted in batch mode to determine Cr(III) binding to the resin sites in the absence or presence of EPS. To develop ion-exchange isotherms for Cr sorption to the resin sites in the absence of EPS, experiments were conducted at a pH of 3 or 4, an ionic strength of 0.01 M NaCl and with $Cr(III)_T$ concentration ranging from 10^{-6} to 10^{-4} M. The amount of the resin in each sample was varied between 0.08 to 0.9 g L^{-1}. The experiments were performed using 50 mL polycarbonate Oak Ridge type centrifuge tubes with a total solution volume of 30 mL. All experiments were performed in the dark at ambient pressure, atmospheric composition and temperature (24 ± 2 °C). The tubes were then placed on a shaker table in the dark for 48 h. Kinetic experiments (data not shown) suggest that this time was sufficient to attain equilibrium in our experiments. After equilibration, the sample pH was checked, the resin was then allowed to settle for 30 min and the supernatant liquid was collected for analysis. The aqueous Cr concentration was determined using ICP-MS (Agilent 7500ce) with a detection limit of 4.06×10^{-10} M, and the Cr bound to the resin was calculated from the difference between the Cr concentration in these samples and the Cr concentration prepared without resin.

The experimental method to develop ion-exchange isotherms for Cr sorption to the resin sites in the presence of microbial EPS

follows the same procedure as described above. The amount of resin used in these samples was 0.290 ± 0.015 g L^{-1}, and the concentration of Cr(III) was 10^{-5} M in all samples. The concentration of EPS ranged from 5 to 200 mg L^{-1}. In all experiments, first, a 4 mL UV-water was added to the tubes, followed by the addition of 0.3 mL of 1 M NaCl for ionic strength adjustment. The pH of the suspension was checked, and adjusted to pH 4 with the addition of NaOH or HCl. After pH adjustments, aliquots of organic ligands were added to obtain the final desired EPS concentration, the pH was checked again, and if necessary, adjusted to pH 4. Following the addition of EPS, aliquots of Cr(III) were added to the tubes to obtain the final desired Cr concentration, and then the pH of the suspension was re-checked and re-adjusted to the desired pH value if necessary. Finally, sufficient UV-water was added to the tubes to bring all the samples to nearly 30 mL. At the end of the equilibration period, the sample pH was checked, and the samples were processed in the same manner as the samples without EPS, as previously described.

2.4. Modeling proton and Cr(III) binding by EPS

In our model, the chemical behavior of microbial EPS was described using a discrete ligand approach as implemented by Westall et al. (1995). Our main goal in using such a simple model was to accurately describe Cr–EPS interactions over a range of environmental conditions (e.g., pH, EPS concentration) by using a minimum number of adjustable parameters. In addition, the modeling approach used in the study provides a consistent evaluative framework for the simulations of interactions of EPS with soil surfaces and ions in speciation (e.g., SCM) and reactive transport models despite the fact that it may not correspond to a strict physical or chemical model of EPS due to complexity and polyfunctionality of EPS. As suggested by Westall et al. (1995), modeling complex systems requires simplification, and a chemically 'reasonable' model, even though a simplification of the target system, should be able to provide insight to system properties even if the model is not 'microscopically' accurate. In this approach, natural organic acids are represented as 'an assembly' of monoprotic acids (HL_i) with assumed pK_a values and without explicit correction for electrostatic effects:

$$HL_i = H^+ + L_i^- \qquad K_{a(i)} = \frac{[H^+][L_i^-]}{[HL_i]} \tag{1}$$

The effect of the electrolyte concentration (i.e., ionic strength) on the titration curves is accounted for using the single reaction set:

$$Na^+ + L_i^- = NaL_i \qquad K_{Na(i)} = \frac{[NaL_i]}{[L_i^-][Na^+]} \tag{2}$$

The chromium binding by EPS occurs mainly through functional groups e.g., carboxylic groups:

$$mCr^{3+} + jHL = Cr_mL_j^{(3m-j)} + jH^+ \qquad \beta_{m,j} = \frac{\left[Cr_mL_j^{(3m-j)}\right][H^+]^j}{[HL]^j[Cr^{3+}]^m} \tag{3}$$

where $Cr_mL_j^{(3m-j)}$ is the Cr-ligand complex, and $\beta_{m,j}$ is the conditional stability constant. The chromium binding by EPS can be evaluated using the ion-exchange data. Detailed information regarding metal–organic ligand complexation modeling using the discrete ligand approach can be found elsewhere (e.g., Westall et al., 1995; Harper et al., 2008).

2.5. X-ray absorption near edge structure (XANES) spectroscopy

XANES analysis was performed to determine the oxidation state of the Cr associated with *P. stutzeri* P40 cell wall after microbial reduction of 40 mg L^{-1} Cr(VI). Chromium (VI) was added to cells and the samples were incubated under controlled conditions (e.g., pH 7). Standards consisting of Cr(III)-hydroxide and potassium dichromate were used to determine the edge shift due to change in Cr oxidation state. Samples were placed in an Al sample holder having a cut out geometry of 2 mm H × 15 mm L × 1.5 mm W. They were then sealed in Kapton tape and analyzed on beam line × 10C at the National Synchrotron Light Source (NSLS) in the fluorescence mode using a Lytle detector. The edge energy was calibrated at a K edge of 5989 eV using a Cr metal foil. During data collection the metal foil was placed in the reference channel and run simultaneously with each sample to monitor shifts in the beamline energy.

2.6. Extended X-ray absorption fine structure (EXAFS) spectroscopy

EXAFS was performed to determine the association of Cr with microbial EPS. The spectra were combined and normalized to the edge jump using programs developed at the University of Washington. ATHENA and ARTEMIS software was used to process the spectra through a multi-step data analysis procedure that included background subtraction and Fourier transformation. Chromium (III)–phosphate hydrate (Sigma–Aldrich, MO) was used to obtain fitting parameters for Cr in the bacterial sample.

3. Results

3.1. EPS biochemical characteristics

The biochemical composition of EPSs analyzed shows variations from one strain to another (Supporting information, Table S1). The carbohydrates were the major components of all EPSs investigated with contents ranging from 276 to 706 mg g^{-1}. A study by Freitas et al. (2010) shows that the EPS isolated from *Pseudomonas oleovorans* NRRL B-14682 is a high molecular weight heteropolysaccharide, composed of neutral sugars (e.g., galactose, glucose, mannose and rhamnpse). Similarly, Hung et al. (2005) found that the EPS extracted from *Pseudomonas fluorescens* Biovar II strain contained neutral sugars such as galactose, glucose, ribose, mannose, arabinose and fucose. The protein contents of EPSs ranged from 107 to 244 mg g^{-1} depending on the type of EPS analyzed. Despite the major differences in total carbohydrate and protein contents, all EPSs contained nearly equal concentrations of uronic acids and phosphorus (Table S1, Supporting information). Hung et al. (2005) found that up to 70% of total carbohydrates in EPS isolated from *P. fluorescens* Biovar II were uronic acids.

3.2. Simulation of EPS potentiometric titration data

A non-electrostatic discrete ligand approach was used to describe acid–base characteristics of EPSs, isolated from *P. putida*, *P. aeruginosa* and *P. stutzeri*. This approach has been previously applied to simulate proton binding to other environmental ligands including humic substances (Westall et al., 1995) and alginic acid (Cetin et al., 2009). In this approach, the basic constraint equations for evaluating the titration data are the proton balance:

$$T_H^{calc} = [H^+] - [OH^-] - \sum[L_i^-] - \sum[NaL_i] \tag{4}$$

and the mass balance for ligand, i:

$$T_{HL(i)} = [HL_i] + [L_i^-] + [NaL_i] \tag{5}$$

The experimental value of T_H (i.e., T_H^{exp}) is evaluated as follows:

$$T_H^{exp} = C_a - C_b + T_H^o = \Delta T_H + \Delta T_H^o \tag{6}$$

where C_a and C_b represent the total concentrations of acid and base added to the system, and T_H^o represents the molar concentration of

strong acid or base initially present. Detailed information on the analysis of titration data by non-electrostatic discrete ligand models can be found elsewhere (e.g., Westall et al., 1995; Kantar and Honeyman, 2005; Harper et al., 2008).

Fig. 1 shows the results of the potentiometric titrations of EPS at ionic strengths of 0.01 and 0.1 M NaCl. The results suggest that microbial EPSs are negatively charged under a wide pH range (pH > 3) due to the deprotonation of functional groups such as carboxylic groups. The analysis of titration data given in Fig. 1 with the discrete ligand approach suggests that the accurate description of acid/base characteristics of EPSs can be accomplished using four different monoprotic ligands (HL_1, HL_2, HL_3 and HL_4) with arbitrarily selected pK_a values of 4, 6, 8 and 10, respectively. The concentration of each of these individual functional groups can be obtained by simultaneously fitting the titration data for each ionic strength as given in Fig. 1. Table 1 shows the adjustable parameters with their optimized values. Here, the goal was a parsimonious model fit to the data to derive a model with a minimum number of discrete ligands to accurately describe acid–base properties of EPS under a wide range of experimental conditions.

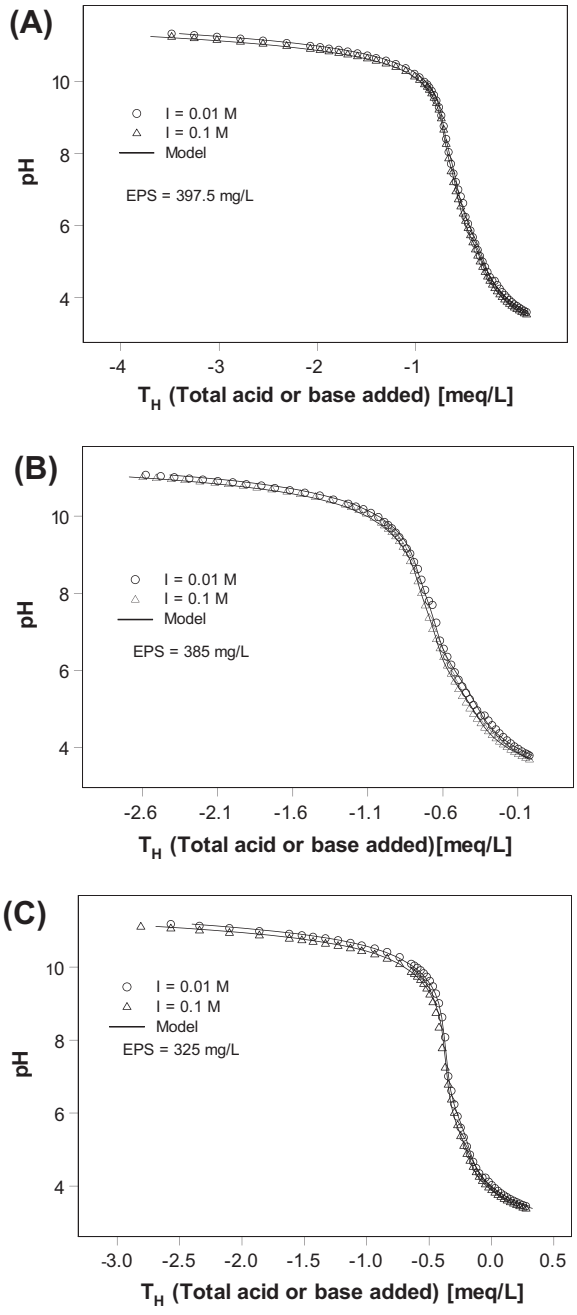

Fig. 1. Acid–base titrations of EPS in 0.01 and 0.1 M NaCl. (A) *P. aeruginosa* P16 (397.5 mg L^{-1}), (B) *P. putida* P18 (385 mg L^{-1}), and (C) *P. stutzeri* P40 (325 mg L^{-1}). Experimental and model fit values of total acid or base added (meq L^{-1}) are plotted vs. pH. Model fits represent the discrete ligand, non-electrostatic approach.

3.3. Simulation of ion-exchange data for Cr(III)–EPS complexation

Once the acid/base characteristics of EPSs were established, the second step in modeling was to simulate Cr binding by EPS through optimization of the results of the ion-exchange experiments at $Cr(III)_T = 1.0 \times 10^{-5}$ M, $I = 0.01$ M NaCl and pH = 4. Fig. 2 shows the results of ion-exchange experiments for Cr(III)–EPS system plotted in terms of Cr(III) sorbed to resin (M) vs. EPS concentration (meq L^{-1}). The simulations contain all possible hydrolysis reactions for chromium (Table 2), the acid–base reactions for each of

Table 1
Acid/base EPS reactions.

Reaction	T_{HLi} (mmol g^{-1})[a]	Log K (I = 0)
P. stutzeri P40[b]		
$HL_1 = L_1^- + H^+$	0.546 ± 0.012	−4
$HL_2 = L_2^- + H^+$	0.538 ± 0.009	−6
$HL_3 = L_3^- + H^+$	0.122 ± 0.011	−8
$HL_4 = L_4^- + H^+$	0.592 ± 0.016	−10
$L_i^- + Na^+ = NaL_i$		1.195
P.putida P18[c]		
$HL_1 = L_1^- + H^+$	0.959 ± 0.016	−4
$HL_2 = L_2^- + H^+$	0.715 ± 0.009	−6
$HL_3 = L_3^- + H^+$	0.356 ± 0.013	−8
$HL_4 = L_4^- + H^+$	0.626 ± 0.016	−10
$L_i^- + Na^+ = NaL_i$		1.006
P. aeruginosa P16[d]		
$HL_1 = L_1^- + H^+$	0.773 ± 0.011	−4
$HL_2 = L_2^- + H^+$	0.673 ± 0.008	−6
$HL_3 = L_3^- + H^+$	0.380 ± 0.012	−8
$HL_4 = L_4^- + H^+$	0.254 ± 0.017	−10
$L_i^- + Na^+ = NaL_i$		0.727

[a] Determined from FITEQL simulation of titration data given in Fig. 1 A,B,C.
[b] Total HL(i) = 1.798 ± 0.012 mmol g^{-1}; T_H^o = 277 μM.
[c] Total HL(i) = 2.656 ± 0.014 mmol g^{-1}; T_H^o = −23.17 μM.
[d] Total HL(i) = 2.080 ± 0.012 mmol g^{-1}; T_H^o = 131 μM.

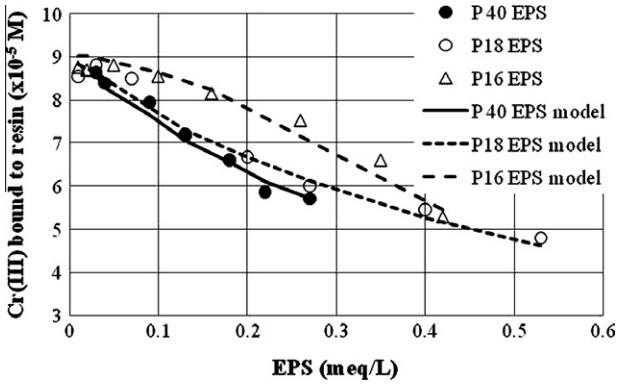

Fig. 2. FITEQL model representation of Cr(III)–EPS binding ion-exchange data plotted as the concentration of chromium bound to the resin (M) vs. EPS concentration (meq L^{-1}). The EPS concentrations were converted from mg L^{-1} to meq L^{-1} using total EPS concentrations ($T_{HL(i)}$) of 1.798, 2.656 and 2.08 mmol g^{-1} for *P. stutzeri* P40, *P. putida* P18, and *P. aeruginosa* P16, respectively (Table 2). The solid lines represent the model fit to reactions given in Table 3 using the discrete ligand approach.

Table 2
Chromium (III) hydrolysis reactions.

Reaction	Log K (I = 0)	Reference
$Cr^{3+} + H_2O = Cr(OH)^{2+} + H^+$	−3.486	Cetin et al. (2009)
$Cr^{3+} + 2H_2O = Cr(OH)_2^+ + 2H^+$	−10.4	Pettit and Powell (1995)
$Cr^{3+} + 3H_2O = Cr(OH)_3 + 3H^+$	−18.7	Pettit and Powell (1995)
$Cr^{3+} + 4H_2O = Cr(OH)_4^- + 4H^+$	−27.8	Pettit and Powell (1995)

EPS ligands shown in Table 1 and the Cr-resin ion exchange reaction given below:

$$Na_3R + Cr^{3+} = CrR + 3Na^+ \qquad K_{CrR} = \frac{[Na^+]^3[CrR]}{[Na_3R][Cr^{3+}]} \tag{7}$$

where R represents the negatively charged network of the cation exchanger. In our previous study, Cetin et al. (2009) determined the value of equilibrium constant (Log K_{CrR} = −1.888) for Reaction (7) by simulating the ion-exchange data for Cr sorption to resin conducted at pHs 3 and 4, and an ionic strength of 0.01 M NaCl. Here, resin site concentrations were converted from g L^{-1} to mol L^{-1} based on a resin exchange capacity of 5.01 mmol g^{-1}, as estimated by Cetin et al. (2009).

A systematic evaluation of complexes between the model ligands (HL_1, HL_2 HL_3 and HL_4) and the dominant Cr(III) species such as Cr^{3+} and $CrOH^{2+}$ was performed, invoking the formation of 1:1 and 1:2 complexes between Cr(III) and two of the same ligand and/or two different ligands. The binding of Cr(III) to HL_1 was examined first, followed by Cr(III) binding to each of the next three ligands. Using mass balance and mass action constraints imposed by the chemical equilibrium model, FITEQL adjusts the binding constant for the postulated complexation reaction(s) until the difference between calculated results and experimental data is minimized. In our simulations, the goodness of fit was checked by WSOS/DF (weighted sum of squares/degrees of freedom). Simulations of Cr(III) binding to HL_1 and HL_2 simultaneously, followed by HL_1 and HL_3 simultaneously, etc., were performed and the fit statistics were noted. The best fit to the experimental ion-exchange data with FITEQL was obtained by postulating a 1:1 complex between HL_2 and Cr(III) for *P. putida* P18 EPS, a 1:1 complex between HL_3 and Cr(III) for *P. stutzeri* P40 EPS, and a 1:2 complex between HL_2 and Cr(III) for *P. aeruginosa* P16 EPS. The conditional stability constants for the complexation reactions are presented in Table 3, and the simulation fits are shown in Fig. 2. The errors estimated on the stability constants include propagated uncertainties based on 2σ errors in Cr analysis (±2%) and pH measurements (±0.01 pH units) (Cetin et al., 2009). A detailed explanation of error estimates can be found in Herbelin and Westall (1999).

4. Discussion

Remediation of subsurface systems contaminated with Cr(VI) can be accomplished through microbial reduction of Cr(VI) by some bacteria e.g., *Pseudomonas*. Chromium (VI) reduced by bacteria usually exists as Cr(III) as indicated by X-ray Near Edge Spectroscopy (XANES) analysis given in Fig. S1 (Supporting information). The results also show that a portion of chromium reduced was retained by the cell wall. However, it is known that toxic substances such as Cr(VI) may stimulate the release of exopolymeric substances (EPS) from bacteria during microbial Cr(VI) reduction (Kilic and Donmez, 2008). The release of such complexing ligands may lead to the mobilization of chromium in subsurface environment due to the formation of highly soluble and less sorbing Cr-ligand complexes (Kantar et al., 2010). Despite the fact that EPS is ubiquitous in natural and engineered systems (Guibaud et al., 2005; Guibaud et al., 2008), their role on Cr(III) speciation, solubility and transport behavior is not clearly established in the literature.

Table 1 shows that a minimum of four different monoprotic ligands was required to accurately describe the acid–base behavior of EPSs isolated from *P. putida, P. aeruginosa* and *P. stutzeri*. This indicates that there are multiple functional groups in all EPSs analyzed. The four ligands invoked, HL_1, HL_2, HL_3 and HL_4 with pK_a values of 4, 6, 8 and 10, respectively can operationally be defined as carboxyl (HL_1), phosphoric/carboxyl (HL_2), phosphoric (HL_3) and hydroxyl/amin/phenolic (HL_4) based on their pK_a values. Liu and Fang (2002) reported on the electrostatic characteristics of binding sites of microbial EPS, and their results indicate presence of carboxylic groups at pK_a values of 4.4–4.8; carboxylic/phosphoric groups at a pK_a value of 6; phosphoric groups at pK_a values of 7.0–7.4 and hydroxyl groups at a pK_a of 11. Similarly, Harper et al. (2008) found that the EPSs isolated from *P. fluorescens, Clostridium* sp. and *S. putrefaciens* exhibited similar polyprolytic behavior with pK_a values ranging from 4 to 8. Guibaud et al. (2005) found that the EPS produced from axenic culture bacterial cells were accurately described using only two apparent pK_a values from 6.8 to 10.1. Similar functional groups can also be found on bacterial cell walls. For example, using a surface complexation model, Fein et al. (1997) observed that the acid/base properties of the cell wall of *Bacillus subtilis* were best described by invoking three distinct types of surface acid functional groups with pK_a values of 4.82, 6.9 and 9.4.

The distribution of the ligands as a function of their pK_a values is shown in Fig. S2 (Supporting information). The total concentration of functional groups in EPS (total HL_i) decreases in the order of *P. putida* P18 (2.656 mmol g^{-1}) > *P. aeruginosa* P16 (2.080 mmol g^{-1}) > *P. stutzeri* P40. (1.798 mmol g^{-1}) (Table 1). These are in the range reported for the EPSs extracted from bacteria in the literature. For example, Guibaud et al. (2005) observed that the EPS isolated from pure bacteria strains displayed multifunctional behavior with proton exchange capacities ranging from 1.7 to 3.5 mmol g^{-1} depending on the type of bacterial culture. Similarly, using a Donnan electrostatic approach, Lamelas et al. (2006) estimated a total functional group concentration of 2.51 mmol g^{-1} for the EPS extracted from *Rhizobium meliloti*. As shown in Fig. S2 (Supporting information), carboxylic groups (HL_1 and HL_2) are the main functional groups of all EPSs analyzed. This result is in good agreement with the EPS components as given in Table S1 (Supporting information). As indicated by Liu and Fang (2002), the carboxylic groups can be found in EPS components such as protein, uronic acid and amino sugars. The EPSs extracted from *P. aeruginosa* P16 and *P. putida* P18 contain much higher phosphoric acid sites (HL_3) compared to the EPS isolated from *P. stutzeri* P40. This coincides well with the measured P contents of EPSs (Supporting information, Table S1). The phosphoric sites are usually associated with the nucleic acids in EPS (Liu and Fang, 2002). Fig. S2 also provides a comparison of microbial EPSs with humic substances e.g., humic acid. Although microbial EPSs contain multiple functional ranging from carboxylic to phosphoric sites, they are less complex, and contain fewer functional groups than fulvic and humic acids, as also suggested by Lamelas et al. (2006) and Harper et al. (2008).

Table 3
Formation constants for Cr(III)–EPS complexes.

EPS	Reaction	Log K (I = 0)[a]	WSOS/DF
P. aeruginosa P16	$Cr^{3+} + 2HL_2 = Cr(L_2)_2^+ + 2H^+$	1.199 ± 0.058[b]	0.527
P. putida P18	$Cr^{3+} + HL_2 = Cr(L_2)^{2+} + H^+$	1.225 ± 0.029[b]	2.054
P. stutzeri P40	$Cr^{3+} + HL_3 = Cr(L_3)^{2+} + H^+$	1.994 ± 0.045[b]	0.247

[a] Errors on stability constants include propagated uncertainties based on 2σ errors in Cr analysis (±2 %) and pH measurements (±0.01 pH units).
[b] Determined from FITEQL simulation of ion-exchange data given in Fig. 2 using the discrete ligand approach.

The analysis of ion-exchange data using the discrete ligand approach suggests that the carboxylic and phosphoric sites are the primary binding sites for Cr(III) under the experimental conditions studied (e.g., pH 4). While chromium (III) strongly complexes with the HL_2 sites (pK_a 6) from the EPSs extracted from *P. putida* P18 and *P. aeruginosa* P16, Cr(III) forms a 1:1 Cr-ligand complex with HL_3 sites (pK_a 8) from the EPS isolated from *P. stutzeri* P40, indicating the phosphoric sites solely play a major role in Cr complexation. The EXAFS analysis performed in the current study provides further evidence on Cr(III)–EPS complexation. For example, the EXAFS results of the fitting for Cr(III)–phosphate and Cr associated with *P. stutzeri* P40 EPS are presented in Fig. 3 and Table S2 (Supporting information). The fitting parameters for Cr(III) phosphate indicate there are 5.7 ± 0.7 O atoms surrounding the octahedral Cr at 1.97 ± 0.01 Å. There are also 4.0 ± 1.3 P atoms at a distance of 3.11 ± 0.5 Å, indicating they are present as phosphate form with the Cr. The Cr associated *P. stutzeri* EPS had 6.0 ± 1.1 O atoms in the Cr inner sphere and 3.8 ± 1.6 P atoms at 3.08 ± 0.04 Å, confirming the predictions of the discrete ligand model that the Cr is associated with the P40 EPS as Cr(III)–phosphate. These results also agree well with the literature data. For instance, studies by Guibaud et al. (2006) and Lamelas et al. (2006) show that carboxylic and phosphoric groups were the primary functional groups for complexation with metal ions e.g., Cd^{2+}. Similarly, studies performed with native (EPS-covered) and EPS-free bacterial cell walls indicate that similar functional groups are involved in metal ion complexation (Boyanov et al., 2003). In an EXAFS study with *Bacillus licheniformis* S-86, Tourney et al. (2009) found that Zn complexation to both native and EPS-free cells was predominantly to carboxyl (p*K*a 5.3–5.4) and phosphate (pK_a 7.4–7.5) functional groups. Fein et al. (1997) observed that both the carboxylic and phosphate sites contributed to metal uptake by the cell walls of *B. subtilis* through the formation of 1:1 Cd-surface complexes between Cd^{2+} and deprotonated surface functional groups (e.g., R–PO–Cd^{+}). The data obtained by Fowle et al. (2000), on the other hand, show that modeling U sorption by the cell walls of *B. subtilis* requires two separate reactions, with the uranyl ion forming surface complexes with the neutral phosphate functional groups (R–POH–UO_2^{2+}) and the deprotonated carboxyl functional groups (R–COO–UO_2^{+}) of the bacterial cell wall.

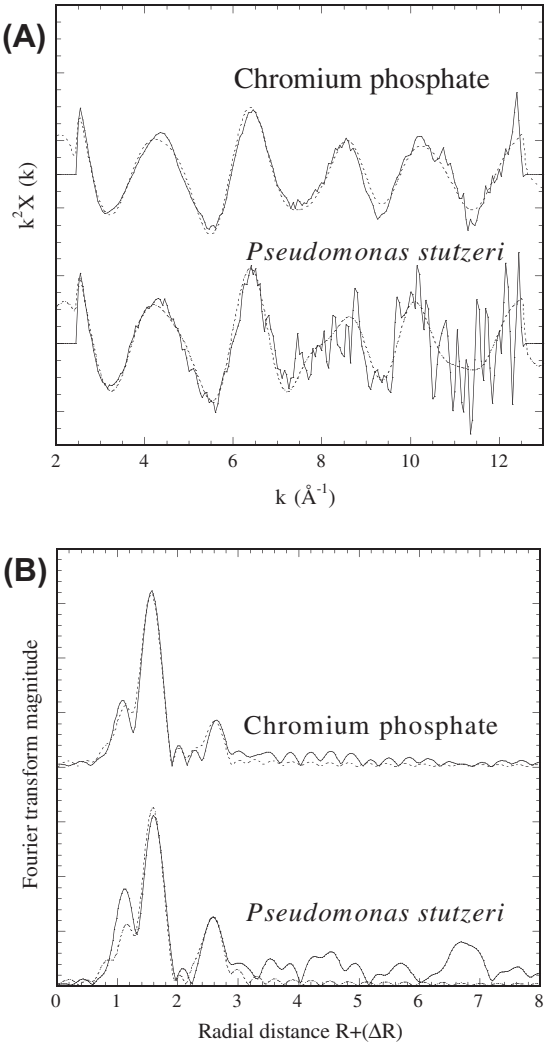

Fig. 3. The fitted k^2-weighted (2.5–12.5 Å) (A) and Fourier transformed spectra (B) showing association of Cr(III)–phosphate and Cr(III) with *P. stutzeri* P40 EPS. Experimental data (-); fitted data (—).

An interesting aspect of modeling is that the affinity of EPS for interacting with the background electrolyte ion (Na^+) decreases in the order of *P. stutzeri* P40 (Log K_{Na} = 1.195) > *P. putida* P18 (Log K_{Na} = 1.006) > *P. aeruginosa* P16 (Log K_{Na} = 0.727) (Table 1), as was the case with Cr(III) binding data (Fig. 2). This indicates that microbial EPS may complex with metal ions in a similar fashion. Note that a single $K_{Na(i)}$ was used to account for the effect of ionic strength on Cr binding to EPS based on the assumption that all EPS functional groups interact with background ions similarly as also indicated by Westall et al. (1995). Westall et al. (1995) have investigated the complexation of Co(II) with leonardite humic acid (LHA), and found that the deprotonated LHA sites were predominantly sodium bound at 0.1 M Na^+ concentration in solution.

4.1. Environmental implications

The microbial EPS released by bacteria during microbial Cr(VI) reduction may strongly complex with chromium (III) depending on the environmental conditions (e.g., pH). The formation of such Cr-organic ligand complexes may have a pronounced impact on Cr speciation, solubility, sorption and transport behavior in subsurface systems. For example, Fig. 4 shows the influence of 50 mg L^{-1} *P. aeruginosa* P16 EPS on 10^{-5} M Cr(III) speciation as a function of pH. Note that Cr(III) speciation is dominated by the Cr–EPS complex under a wide pH range.

5. Conclusions

The conditional stability constants for Cr(III) complexing with EPS, isolated from *P. putida* P18, *P. aeruginosa* P16 and *P. stutzeri*

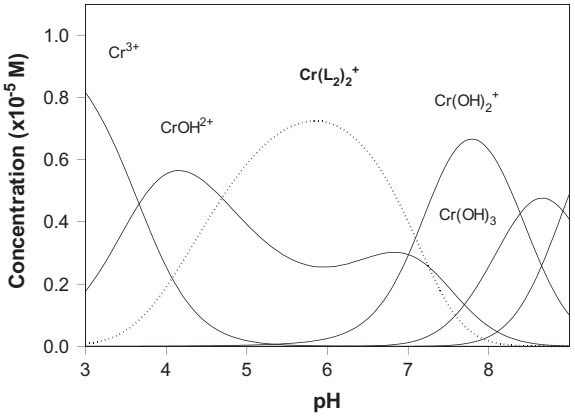

Fig. 4. Distribution of solution-phase Cr(III) species in equilibrium with air (P_{CO2} = $10^{-3.5}$ atm) as a function of pH, including the Cr-P16 EPS complex for $Cr(III)_T$ = 10^{-5} M and *P. aeruginosa* P16 EPS = 50 mg L^{-1}. The equilibrium constants for Cr hydrolysis are from Table 2.

P40 cultures, were determined at pH 4 and an ionic strength of 0.01 M NaCl using an ion-exchange technique and potentiometric titrations. Spectroscopic techniques (EXAFS) were also used to evaluate the nature of Cr binding by EPS. The data from ion-exchange experiments and potentiometric titrations were analyzed using a non-electrostatic discrete ligand approach in FITEQL. The analysis of titration data with the discrete ligand model shows that the acid–base characteristics of the three microbially produced EPSs can be adequately described by invoking four different monoprotic acid functional groups with arbitrarily assigned pK_a values of 4, 6, 8 and 10. Despite the similarities in functional groups, the total concentration of functional groups in EPS (total HL_i) decreases in the order of *P. putida* P18 (2.656 mmol g^{-1}) > *P. aeruginosa* P16 (2.080 mmol g^{-1}) > *P. stutzeri* P40. (1.798 mmol g^{-1}), indicating that the functional group composition may vary from one strain to another.

The analysis of ion-exchange data with the discrete ligand model suggests that the Cr(III) binding by EPS isolated from *P. putida* P18 and *P. stutzeri* P40 can be described based on a reaction stoichiometry of 1:1 Cr(III)-ligand complexes. However, the accurate description of Cr binding by EPS from *P. aeruginosa* P16 requires postulation of a 1:2 complex between Cr(III) and EPS ligands under the experimental conditions studied (e.g., pH 4). The results also show that only the pK_a 6 (L_2) and 8 (L_3) ligands are sufficient to accurately simulate the Cr(III)/EPS binding. This implies that the carboxyl and/or phosphoric acid groups in EPS are the primary binding sites for complexing with Cr(III) under the experimental conditions examined (e.g., pH 4). The EXAFS analysis provides further evidence that the EPSs isolated from bacteria e.g., *P. stutzeri* complex with Cr(III) through phosphate sites.

Acknowledgments

The financial support for the present study was provided by the Scientific and Technical Research Council of Turkey (TUBITAK) (Project # 105Y272) and Mersin University (BAP-FBE CM (HD) 2008-2. The authors also thank the reviewers of the manuscript for their considerable time and thoughtfulness put into their reviews.

Appendix A. Supplementary data

Supplementary data associated with this article can be found, in the online version, at doi:10.1016/j.chemosphere.2011.01.009.

References

Aquino, S.F., Stuckey, D.C., 2004. Soluble microbial products formation in anaerobic chemostats in the presence of toxic compounds. Water Res. 38, 255–266.

Boyanov, M.I., Kelly, S.D., Kemner, K.M., Bunker, B.A., Fein, J.B., Fowle, D.A., 2003. Adsorption of cadmium to *Bacillus subtilis* bacterial cell walls: a pH-dependent X-ray absorption fine structure spectroscopy study. Geochim. Cosmochim. Acta 67 (18), 3299–3311.

Cetin, Z., Kantar, C., Alpaslan, M., 2009. Interactions between uronic acids and chromium (III). Environ. Toxicol. Chem. 28 (8), 1599–1608.

Comte, S., Guibaud, G., Baudu, M., 2008. Biosorption properties of extracellular substances (EPS) towards Cd, Cu and Pb for different pH values. J. Hazard. Mater. 151, 185–193.

Fein, J.B., Daughney, C.J., Yee, N., Davis, T.A., 1997. A chemical equilibrium model for metal adsorption onto bacteria surfaces. Geochim. Cosmochim. Acta 61 (16), 3319–3328.

Fowle, D.A., Fein, J.B., Martin, A.M., 2000. Experimental study of uranyl adsorption onto *Bacillus subtilis*. Environ. Sci. Technol. 34, 3737–3741.

Freitas, F., Alves, V.D., Pais, J., Carvalheira, M., Costa, N., Oliveira, R., Reis, M.A.M., 2010. Production of a new exopolysaccharide (EPS) by *Pseudomonas oleovorans* NRRL B-14682 grown on glycerol. Process Biochem. 45 (3), 297–305.

Guibaud, G., Tixier, N., Bouju, A., Baudu, M., 2003. Relation between extracellular polymers composition and its ability to complex Cd, Cu and Pb. Chemosphere 52, 1701–1710.

Guibaud, G., Comte, S., Bordas, F., Dupuy, S., Baudu, M., 2005. Comparison of the complexation potential of extracellular polymeric substances (EPS), extracted from activated sludges and produced by pure bacteria strains, for cadmium, lead and nickel. Chemosphere 59, 629–638.

Guibaud, G., van Hullebusch, E., Bordas, F., 2006. Lead and cadmium biosorption by extracellular polymeric substances (EPS) extracted from activated sludges: pH sorption edge tests and mathematical equilibrium modeling. Chemosphere 64, 1955–1962.

Guibaud, G., Bordas, F., Saaid, A., D'abzac, P., van Hullebusch, E., 2008. Effect of cadmium and lead binding by extracellular polymeric substances (EPS) extracted from environmental bacterial strains. Colloids Surf. B Biointerfaces 63, 48–54.

Harper, R.M., Kantar, C., Honeyman, B.D., 2008. Binding of Pu (IV) to galacturonic acid and extracellular polymeric substances (EPS) from *Shewanella putrefaciens, Clostridium* sp. and *Pseudomonas fluorescens*. Radiochim. Acta 96, 753–762.

Hartree, E.F., 2004. Determination of protein: a modification of the lowry method that gives a linear photometric response. agricultural research council. Unit Reprod. Physiol. Biochem., 307.

Herbelin, A.L., Westall, J.C. 1999. FITEQL, A Computer Program for Determination of Chemical Equilibrium Constants from Experimental Data. Rep. 96-01, Oregon State University, Corvallis, USA.

Hung, C.C., Santschi, P.H., 2001. Spectrophotometric determination of total uronic acids in sea-water using cation exchange separation and pre-concentration by lyophilization. Anal. Chim. Acta 427, 111–117.

Hung, C.C., Santschi, P.H., Gillow, J.B., 2005. Isolation and characterization of extracellular polysaccharides produced by *Pseudomonas fluorescens* Biovar II. Carbohydr. Polym. 61, 141–147.

Kantar, C., Honeyman, B.D., 2005. Plutonium (IV) complexation with citric and alginic acids at low Pu_T concentrations. Radiochim. Acta 93 (12), 757–766.

Kantar, C., Demiray, H., Dogan, N.M., 2010. Role of microbial exopolymeric substances (EPS) on chromium sorption and transport in heterogeneous subsurface soil. II. Binding of Cr(III) in EPS/soil system. Chemosphere, doi: 10.1016 /j.chemosphere.2010.11.001.

Kilic, N.K., Donmez, G., 2008. Environmental conditions affecting exopolysaccharide production by *Pseudomonas aeruginosa*, *Micrococus* sp. and *Ochrobactrum* sp.. J. Hazard. Mater. 154 (1–3), 1019–1024.

Kurbatov, M.H., Wood, G.B., Kurbatov, J.D., 1951. Isothermal adsorption of cobalt from dilute solutions. J. Phys. Chem. 55, 1170–1182.

Lamelas, C., Benedetti, M., Wilkinson, K.J., Slaveykova, V.I., 2006. Characterization of H^+ and Cd^{2+} binding properties of the bacterial exopolysaccharides. Chemosphere 65 (8), 1362–1370.

Liu, H., Fang, H.H.P., 2002. Characterization of electrostatic binding sites of extracellular polymers by linear programming: analysis of titration data. Biotechnol. Bioeng. 80, 806–811.

Pettit, L.D., Powell, H.K.J., 1995. IUPAC Stability Constants Database. Version 2. 61. Academic, Software, Otley, UK.

Priester, J.H., Olson, S.G., Webb, S.M., Neu, M.P., Hersman, L.E., Holden, P.A., 2006. Enhanced exopolymer production and chromium stabilization in *Pseudomonas putida* unsaturated biofilms. Appl. Environ. Microbiol. 72 (3), 1988–1996.

Puzon, G.J., Roberts, A.G., Kramer, D.M., Xun, L., 2005. Formation of soluble organo-chromium(III) complexes after chromate reduction in the presence of cellular organics. Environ. Sci. Technol 39, 2811–2817.

Ruzic, I., 1996. Trace metal complexation at heterogeneous binding sites in aquatic systems. Mar. Chem. 53, 1–15.

Schubert, J., 1948. The use of ion exchangers for the determination of physical chemical properties of substance particularly radiotracers in solution. I. Theoretical. J Phys Colloid Chem 52, 340–346.

Sheng, G-P., Yu, H-Q., Yue, Z-B., 2005. Production of extracellular polymeric substances from *Rhodopseudomonas acidophila* in the presence of toxic substances. Appl. Microbiol. Biotechnol. 69, 216–222.

Smith, G.C., Rees, T.F., MacCarthy, P., Daniel, S.R., 1986. On the interpretation of Schubert plot slopes for metal-humate systems. Soil Sci. 141 (1), 7–9.

Southgate, D.A.T., 1976. Determination of Food Carbohydrates. Applied Science Publishers Ltd., England. p. 108.

Tourney, J., Ngwenya, B.T., Mosselmans, J.W.F., Magennis, M., 2009. Physical and chemical effects of extracellular polymers (EPS) on Zn adsorption to *Bacillus licheniformis* S-86. J. Colloid Interface Sci. 337, 381–389.

Westall, J.C., Jones, J.D., Turner, G.D., Zachara, J.M., 1995. Models for association of metals with heterogeneous sorbents. 1. Complexation of Co(II) by leonardite humic acid as a function of pH and $NaClO_4$ concentration. Environ. Sci. Technol. 29, 951–959.